THE JOURNAL OF BIOLOGICAL CHEMISTRY VOL. 285, NO. 53, pp. 41896–41910, December 31, 2010

Protein Kinase C δ-specific Activity Reporter Reveals Agonist-evoked Nuclear Activity Controlled by Src Family of Kinases*[S]◆

Received for publication, September 10, 2010, and in revised form, October 18, 2010 Published, JBC Papers in Press, October 19, 2010, DOI 10.1074/jbc.M110.184028

Taketoshi Kajimoto[‡§], Seishiro Sawamura[§], Yumi Tohyama[¶], Yasuo Mori[§], and Alexandra C. Newton[‡1]

From the [‡]Department of Pharmacology, University of California at San Diego, La Jolla, California 92093, the [§]Department of Synthetic Chemistry and Biological Chemistry, Kyoto University, Kyoto-daigaku Katsura, Nishikyo-ku, Kyoto 615-8510, Japan, and the [¶]Division of Biochemistry, Faculty of Pharmaceutical Sciences, Himeji Dokkyo University, 7-2-1 Kamiohno, Himeji, Hyogo 670-8524, Japan

Conventional and novel protein kinase C (PKC) isozymes transduce the abundance of signals mediated by phospholipid hydrolysis; however redundancy in regulatory mechanisms confounds dissecting the unique signaling properties of each of the eight isozymes constituting these two subgroups. Previously, we created a genetically encoded reporter (C kinase activity reporter (CKAR)) to visualize the rate, amplitude, and duration of agonist-evoked PKC signaling at specific locations within the cell. Here we designed a reporter, δCKAR, that specifically measures the activation signature of one PKC isozyme, PKC δ, in cells, revealing unique spatial and regulatory properties of this isozyme. Specifically, we show two mechanisms of activation: 1) agonist-stimulated activation at the plasma membrane (the site of most robust PKC δ signaling), Golgi, and mitochondria that is independent of Src and can be triggered by phorbol esters and 2) agonist-stimulated activation in the nucleus that requires Src kinase activation and cannot be triggered by phorbol esters. Translocation studies reveal that the G-protein-coupled receptor agonist UTP induces the translocation of PKC δ into the nucleus by a mechanism that depends on the C2 domain and requires Src kinase activity. However, translocation from the cytosol into the nucleus is not required for the Src-dependent regulation of nuclear activity; a construct of PKC δ prelocalized to the nucleus continues to be activated by UTP by a mechanism dependent on Src kinase activity. These data identify the nucleus as a signaling hub for PKC δ that is driven by receptor-mediated signaling pathways (but not phorbol esters) and differs from signaling at plasma membrane and Golgi in that it is controlled by Src family kinases.

Protein kinase C δ (PKC δ) distinguishes itself in the 10-member family of PKC isozymes by having a defined nuclear function (1–3). Specifically, this isoform translocates to the nucleus in response to apoptotic stress, an event that promotes cell death. This contrasts from other PKC isozymes, which function primarily at membranes and protein scaffolds outside the nucleus and which generally have pro-survival functions (2). Elegant studies by Reyland and co-workers (4, 5) have established that apoptotic stimuli cause phosphorylation of PKC δ on 2 Tyr residues in the regulatory domain, modifications that allow a nuclear localization sequence (NLS)[2] on PKC δ to drive this isozyme into the nucleus. Its phosphorylation on Tyr and its presence in the nucleus are required for PKC δ to induce apoptosis in response to chemotherapeutics and other apoptosis-inducing agents such as ceramide and etoposide (1, 4–10). Direct activation of PKC δ is also the mechanism by which phorbol esters exert their apoptotic effects in certain cell types (rather than the more common effect of phorbol esters in promoting survival and proliferation) (7, 11, 12). This phorbol ester-mediated activation of PKC δ has been particularly well characterized in the LNCaP prostate cancer cells, where most recently a requirement for translocation to the plasma membrane has been identified as a key step in the phorbol ester-mediated activation of PKC δ (13). Thus, direct activation of PKC δ by binding phorbol esters mediates apoptosis via a mechanism requiring plasma membrane translocation of the enzyme, whereas activation triggered by DNA-damaging agents such as etoposide mediate apoptosis via a Tyr kinase-dependent nuclear translocation. Whether PKC δ is activated in the nucleus following normal agonist-evoked signaling and, if so, how much of the signaling output of PKC δ derives from nuclear activity *versus* activity at other cellular locations, such as the plasma membrane, is not known.

The protein kinase C family comprises 10 members, of which eight are activated by the lipid second messenger diacylglycerol (2, 14, 15). Diacylglycerol recruits conventional and novel PKC isozymes to cell membranes by binding the C1 domain, inducing a conformational change that relieves auto-

* This work was supported, in whole or in part, by National Institutes of Health Grants P01 DK54441 and GM 43154 (to A. C. N.). This work was also supported by a grant-in-aid for Japan Society for the Promotion of Science (JSPS) Fellows from the JSPS, Uehara Memorial Foundation (to T. K.).

◆ This article was selected as a Paper of the Week.

[S] The on-line version of this article (available at http://www.jbc.org) contains supplemental Fig. 1.

[1] To whom correspondence should be addressed: 9500 Gilman Dr. 0721, La Jolla, CA 92093-0721. Tel.: 858-534-4527; Fax: 858-822-5888; E-mail: anewton@ucsd.edu.

[2] The abbreviations used are: NLS, nuclear localization sequence; AKAR, A kinase activity reporter; BKAR, B kinase activity reporter; CKAR, C kinase activity reporter; PdBu, phorbol dibutyrate; DMSO, dimethyl sulfoxide; PP, protein phosphatase.

inhibition and allows downstream signaling of these kinases (16). Conventional PKC isozymes (α, βI, βII, γ) also respond to Ca^{2+}, which facilitates membrane recruitment of this group of isozymes by binding a second membrane-targeting module, the C2 domain. The coordinated regulation by two membrane-targeting modules ensures that conventional PKC isozymes are only activated when both Ca^{2+} and diacylglycerol are generated. Novel PKC isozymes (δ, ϵ, θ, η) are recruited solely via the C1 domain; a single residue change in their C1 domain, from Tyr to Trp, allows these isozymes to have a 2 orders of magnitude higher affinity for diacylglycerol, allowing them to respond to agonist-evoked increases in diacylglycerol in the absence of pretargeting via Ca^{2+} (17). The high levels of diacylglycerol at Golgi favor this surface for signaling by novel PKC isozymes (18). In addition to selectivity in phospholipid interactions, scaffold interactions play an important role in tethering specific isozymes at precise intracellular locations (19). We previously generated a genetically encoded FRET-based reporter, CKAR, that allowed us to determine the signature of activation of bulk PKC at discrete locations within the cell (20–22). However, whether specific isozymes have specific activation signatures that are not discernable in the bulk signal of total PKC output of the cell could not be addressed.

Here we generated a genetically encoded reporter with the same modular structure as the original CKAR but with a unique substrate sequence that allows specific visualization of PKC δ activity in cells. We find that signaling by PKC δ is high at the plasma membrane and modest at the Golgi. Importantly, the natural agonist UTP, but not phorbol esters, causes significant activation of PKC δ in the nucleus. This nuclear activation, unlike the activation observed at the plasma membrane or Golgi, depends on Src activation. This requirement for Src is not solely to bring PKC δ to the nucleus because enzyme pretargeted to the nucleus cannot be activated by UTP in cells pretreated with Src inhibitors. These data unveil the activation signature of PKC δ at specific cellular locations and establish that the nucleus is a major signaling hub for this isozyme.

EXPERIMENTAL PROCEDURES

Materials—Phorbol 12,13-dibutyrate (PdBu), Gö6983, Gö6976, calyculin A, forskolin, PP2, PP3, and UTP were obtained from Calbiochem. EGF was purchased from Upstate Biotech Millipore (Lake Placid, NY). SU6656 was obtained from Sigma-Aldrich. Anti-phospho Par-1B antibody was purchased from Abcam, and anti-GFP antibody and anti-DsRed antibody were obtained from Clontech. Biomax MR film used for Western blot analyses was from Eastman Kodak Co. All other materials were reagent-grade.

Plasmid Constructs—Candidate δ-selective CKAR (δCKAR) constructs were generated through substitution by PCR of the substrate sequence within pcDNA3-CKAR with sequences from PKC δ substrates. Site-directed mutagenesis of δCKAR versions was carried out using the QuikChange protocol (Stratagene, La Jolla, CA). For creating δCKAR-T/A, the phospho-acceptor threonine was mutated to an alanine following the QuikChange protocol. Plasma membrane-δCKAR, Golgi-δCKAR, and mitochondria-δCKAR were generated by fusing in-frame sequences encoding the amino-terminal 7 amino acids of Lyn kinase, the amino-terminal 33 amino acids of endothelial nitric-oxide synthase, or the amino-terminal 33 amino acids of TOM 20, respectively, to the immediate 5′-end of δCKAR (23). Nucleus-δCKAR was generated similarly by fusing to the 3′-end of δCKAR sequences encoding a basic nuclear localization signal, PKKRKVEDA (23). The A kinase activity reporter (AKAR) was a gift from Roger Tsien (University of California at San Diego (UCSD)) (24). The B kinase activity reporter (BKAR) and PKB-RFP were previously generated in this laboratory (25, 26). The red fluorescent-tagged PKCs were generated by subcloning the DNA encoding monomeric red fluorescent protein (mRFP) to that encoding the C terminus of PKC α, PKC βI, PKC βII, PKC γ, PKC δ, PKC ϵ, or PKC ζ. C2-deleted PKC δ-RFP was made by removing the first 126 residues of full-length PKC δ-RFP as described previously (27). Nuc-PKC δ-RFP was generated by fusing to the 3′-end of PKC δ-RFP sequences encoding a basic nuclear localization signal, PKKRKVEDA. PKM ζ-RFP was made by removing the first 184 residues of full-length PKC ζ-RFP. For PKC ζ(A119E)-RFP, alanine 119 was mutated to a glutamate using the QuikChange protocol.

Cell Culture and Transfection—COS7 and HeLa cells were maintained in Dulbecco's modified Eagle's medium (Mediatech, Inc., Manassas, VA) containing 10% fetal bovine serum and 1% penicillin/streptomycin at 37 °C in 5% CO_2. Cells were plated onto sterilized glass coverslips in 35-mm dishes prior to transfection. Transient transfection was carried out using FuGENE 6 (Roche Diagnostics GmbH, Mannheim, Germany). Cells were imaged within 24 h after transfection. For EGF stimulation, cells were serum-starved at least for 24 h after transfection and then imaged.

FRET Imaging—COS7 and HeLa cells were rinsed once with, and imaged in, Hanks' balanced salt solution containing 1 mM Ca^{2+}. Images were acquired on a Zeiss Axiovert microscope (Carl Zeiss, Inc., Jena, Germany) using a MicroMax digital camera (Roper Industries Inc., Sarasota, FL) controlled by MetaFluor software (Universal Imaging Corp. Ltd., Buckinghamshire, UK). Optical filters were obtained from Chroma Technology Corp. (Bellows Falls, VT). Using a 5% neutral density filter, CFP and FRET images were obtained every 15 s through a 420/20-nm excitation filter, a 450-nm dichroic mirror, and a 475/40-nm emission filter (CFP) or 535/25-nm emission filter (FRET). YFP emission was also monitored as a control for photobleaching through a 495/10-nm excitation filter, a 505-nm dichroic mirror, and a 535/25-nm emission filter. Excitation and emission filters were switched in filter wheels (Lambda 10-2; Sutter Instrument Co., Novato, CA). Integration times were 200 ms for CFP and FRET and 100 ms for YFP. Red fluorescent protein (monomeric; RFP) images were obtained through a 568/55-nm excitation filter, a 600-nm dichroic mirror, and a 653/95-nm emission filter.

Imaging Data Analysis—Images were reanalyzed using MetaFluor Analyst (Universal Imaging Corp. Ltd.). One region per cell was selected such that there was no net movement of the targeted reporter in and out of the selected region, and MetaFluor Analyst was used to calculate the average

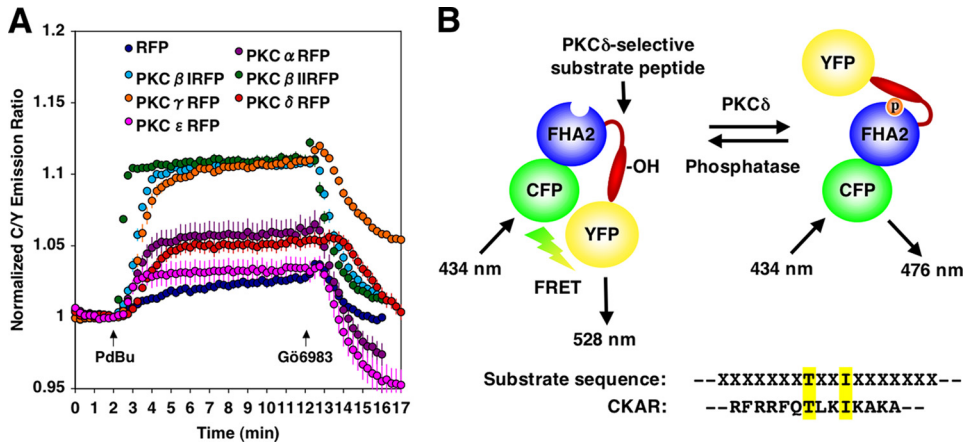

FIGURE 1. **PKC isotype selectivity of CKAR and strategy for developing PKC δCKAR.** *A*, COS7 cells were co-transfected with CKAR and RFP, PKC α-RFP, PKC βI-RFP, PKC βII-RFP, PKC γ-RFP, PKC δ-RFP, or PKC ϵ-RFP. The FRET ratio was quantified following the addition of PdBu (200 nM) and then the specific PKC inhibitor Gö6983 (500 nM). Data represent the average ± S.E. from at least three independent experiments. Data are presented as the emission of CFP over the emission of YFP normalized to that at $t = 0$. *C/Y*, CFP/YFP. *B*, the PKC substrate peptide of CKAR was replaced with PKC δ-selective substrate peptides. δCKAR consists of monomeric CFP, the FHA2 domain of Rad53p, a PKC δ-selective phosphorylation sequence (*red*), and monomeric YFP. In the unphosphorylated state, monomeric CFP and monomeric YFP are in a proximity and an orientation resulting in FRET. Once phosphorylated by PKC δ at the threonine within the substrate sequence (*highlighted* in *yellow*), the FHA2 domain binds the phosphorylated sequence, resulting in a conformational change that alters the FRET ratio. Isoleucine at the P+3 position (*highlighted* in *yellow*) is critical for the binding of phospho-threonine to the FHA2 domain.

FRET ratio within the selected region. Base-line images were acquired for 1–2 min before adding ligand. The corrected data traces were normalized to 1 by dividing by the average base-line FRET ratio, and data from different imaging dishes were referenced around the ligand addition time point. The normalized CFP/YFP emission ratio is representative as the average of these corrected values ± S.E. The CKAR "phosphorylation index" was calculated by summing the normalized CFP/YFP FRET ratio values between the time of the addition of agonist until the time of the addition of inhibitor. Thus, it represents the area under the activation curves. The calculating formula is: CKAR phosphorylation index = $\sum$ ((normalized CFP/YFP FRET ratio (t)) − 1), t = 135–720 s (15-s interval).

Distribution of PKC δ—HeLa cells expressing PKC δ-RFP were rinsed once with, and imaged in, Hanks' balanced salt solution containing 1 mM Ca^{2+}. The fluorescence of RFP was monitored using confocal laser scanning microscopy (LSM 510 META; Carl Zeiss Inc., Jena, Germany) at a 543-nm excitation wavelength with a 560-nm-long pass barrier filter. Differential interference contrast image was obtained using a 488-nm excitation wavelength.

Western Blotting—COS7 cells overexpressing RFP or RFP-tagged PKC constructs were grown to near confluence in 60-mm dishes. Cells were washed once in Hanks' balanced salt solution containing 1 mM Ca^{2+} and treated for the indicated times with 200 nM PdBu at 37 °C. Cells were harvested with lysis buffer (50 mM Na_2HPO_4, 1 mM sodium pyrophosphate, 20 mM NaF, 2 mM EDTA, 2 mM EGTA, 1% Triton X-100, 1 mM DTT, 200 μM benzamidine, 40 μg/ml leupeptin, and 1 mM PMSF). The detergent-solubilized cell lysate was obtained by centrifuging the whole cell lysate in a microcentrifuge at 13,000 rpm for 5 min. In the case of the experiment for constitutively active form of PKC δ, cells were collected 24 h after transfection. The detergent-solubilized lysates were separated on SDS-PAGE gels, and Western blots were analyzed by chemiluminescence.

RESULTS

As a first step to designing an isozyme-specific reporter of PKC δ, we examined whether the originally designed CKAR (20) discriminated between conventional and novel PKC isozymes. COS cells were transfected with CKAR and RFP-tagged constructs of either conventional PKC isozymes (PKC α, PKC βI, PKC βII, or PKC γ) or novel PKC isozymes (PKC δ or PKC ϵ). Cells were then treated with PdBu, and the phosphorylation of the reporter was quantified in cells expressing equivalent amounts of recombinant PKC (quantified from RFP signal). The data in Fig. 1*A* reveal that each isozyme phosphorylated CKAR. The rate of phosphorylation was fairly comparable for the different overexpressed isozymes, with half-times of ~0.5 min for PKC βII, 1 min for PKC α, PKC βI, PKC γ, PKC ϵ, and 1.5 min for PKC δ. However, the amplitude of phosphorylation differed significantly among the isozymes. Because the dynamic range of the reporter does not vary with isozyme (same reporter), the relative increase in amplitude triggered by phorbol esters reflects the level of basal activity of each isozyme (21). Consistent with this, the addition of the PKC inhibitor Gö6983 reversed the phosphorylation of CKAR to well below base line for isozymes with a low amplitude (*e.g.* PKC ϵ, α) and to base line for isozymes with a high amplitude (*e.g.* PKC βI, βII, γ). These data reveal that CKAR is an effective reporter for all PKC isozymes. Moreover, they reveal that some isozymes, most notably PKC ϵ, have unusually high basal activity in cells, whereas others, notably PKC βI, βII, and γ, have very low basal activity.

To tune the activity of CKAR to be selective for PKC δ, we replaced the phosphorylation sequence in CKAR with sequences from known PKC δ substrates, keeping 2 residues invariant: Thr at the phospho-acceptor region (because the phospho-peptide binding module of the reporter, the FHA2 domain, is selective for phospho-Thr over phospho-Ser) and the Ile at the $p + 3$ position (because this is required for the FHA2 domain to bind the phosphorylated sequence) (Fig. 1*B*).

TABLE 1

Candidate sequences of PKC δ selective substrate

Bold letters indicate basic amino acids. Boxes indicate the amino acids mutated from original sequence respectively. Lamin B1: Human lamin B1 (NM_005573). eEF1α-1: human eukaryotic translation elongation factor 1 α 1 (NM_001402). Par-1B α: human Ser/Thr protein kinase Par-1B α (NM_017490). 14–3-3η: human 14–3-3η protein (L20422). TP73: human tumor protein p73 (NM_005427). PLSCR1: human phospholipid scramblase 1 (NM_021105). IRS-1: human insulin receptor substrate 1 (NM_005544). Rel A: rat NF-κB p65 subunit, Rel A (AY307375). IRAP: rat insulin-regulated membrane aminopeptidase (U76997). PKC δ optimal: optimal sequence for PKC δ determined by the peptide library. [Ser[25]]-PKC 19-31: pseudosubstrate sequence of PKC δ with Thr at the phospho-acceptor position [19-31, Ser[25]].

Candidates of	Position																					
PKC δ -selective substrate	-9	-8	-7	-6	-5	-4	-3	-2	-1	0	1	2	3	4	5	6	7	8	9	10	11	12
Lamin B1 (S405)					V	S	**R**	A	S	T	S	**R**	I	V	**R**							
eEF1α-1 (T432)	**R**	F	A	V	**R**	D	M	**R**	Q	T	V	A	I	G	V	I	**K**	A	V	D	**K**	**K**
Par-1B α (T595)			**R**	G	V	S	S	**R**	S	T	F	H	I	G	Q	L	**R**	Q	V	**R**		
14-3-3η (S59)		N	V	V	G	A	**R**	**R**	S	T	W	**R**	I	I	S	S	I	E				
TP73 (S289)		D	G	Q	V	L	G	**R**	**R**	T	F	E	I	**R**	I	C	A	C				
PLSCR1 (T161)		C	C	G	P	S	**R**	P	F	T	L	**R**	I	I	D	N	M	G				
IRS-1 (S24)	**K**	V	G	Y	L	**R**	**K**	P	**K**	T	M	H	I	**R**	F	F	V	L	**R**			
Rel A (S311)				T	Y	E	T	F	**K**	T	I	M	I	**K**	S	P	F					
IRAP (S80)				A	**K**	L	L	G	M	T	F	M	I	**R**	S	S	G					
PKC δ optimal			A	**R**	**R**	**K**	**R**	**K**	G	T	F	F	I	G	G							
[Ser[25]]-PKC 19-31				**R**	F	A	**R**	**K**	G	T	L	**R**	I	**K**	N	V						

We inserted nine sequences from known PKC δ substrates (lamin B1(28), eEF1α-1 (29), Par-1B α (30, 31), 14-3-3η (32), TP73 (33), PLSCR1 (34, 35), IRS-1 (36), RelA (37), IRAP (38), the optimal sequence predicted for PKC δ by oriented peptide libraries (39), and the pseudo-substrate sequence of the enzyme with Thr at the phospho-acceptor site (40) (Table 1). Fig. 2*A* presents the ability of each of these reporters to be phosphorylated in cells by conventional and novel PKC isozymes. To quantitatively assess the selectivity of the different isozymes for each reporter, we normalized the area under the phosphorylation curve for each reporter to the area obtained using the original CKAR. This relative phosphorylation index is presented in Fig. 2*B*. Some sequences were phosphorylated well but non-selectively by all isozymes (notably 14-3-3η), others were not phosphorylated well (notably TP73), and some displayed selectivity for PKC δ (notably eEF1α-1, Par1B α, IRS-1, and the optimal PKC δ sequence). These four sequences produced a CKAR whose phosphorylation index was at least 3-fold greater for PKC δ when compared with other isozymes.

We then varied the amino acids in the Par-1B α and eEF1 α sequences, constructing 25 and 31 different versions, respectively (Table 2). We measured their phosphorylation by PKC δ and PKC βII and selected for CKAR versions in which the phosphorylation index was high and the selectivity for PKC δ over PKC βII was high (Fig. 3). Thus, although Par-1B α version 10 had a high phosphorylation index, it had no selectivity for PKC δ (in fact, it is interesting that just the replacement of Phe with Val at the P-1 position favored phosphorylation by PKC βII). In contrast, Par-1B α version 12 had a moderate phosphorylation index but almost an order of magnitude selectivity for PKC δ over PKC βII. We present the optimization of the Par-1B α sequence because, ultimately, it provided a more selective reporter.

We next tested whether δCKAR Par-1B α version 12 was reading out sequence-specific phosphorylation catalyzed by PKC δ. Fig. 4*A* shows that the reporter responded to overexpressed PKC δ and that this response was abolished when the phospho-acceptor Thr was replaced with Ala. Fig. 4*B* shows that the reporter was not sensitive to PKA activation, in contrast to AKAR (24), which responded robustly to increased cAMP levels induced by forskolin, nor was the reporter sensitive to Akt/PKB activation, in contrast to BKAR (26), which responded robustly to EGF (Fig. 4*C*). Lastly, the PKC δ-dependent phosphorylation of the reporter was abolished by the inhibitor Gö6983, which inhibits all PKC isozymes (Fig. 4*D*, *red circles*) but was insensitive to Gö6976 (Fig. 4*D*, *green circles*), which inhibits conventional but not novel PKC isozymes. These data reveal that δCKAR Par-1B α version 12 provides a specific read-out of PKC δ activity in cells.

We further tested the specificity of δ CKAR Par-1B α version 12 toward seven different PKC isozymes, including the atypical isozyme, PKC ζ. Fig. 5*A* shows that the reporter was highly selective for PKC δ, displaying a phosphorylation index at least 4-fold higher than that of other isozymes, including the novel PKC isozyme, PKC ϵ. As a final measure of selectivity, we analyzed the phosphorylation of δCKAR Par-1B α version 12 in cells overexpressing various PKC isozymes and treated without or with phorbol esters. To this end, we took advantage of an antibody directed against the Par-1B α phosphorylation sequence. Fig. 5*C* shows that the reporter was specifically and robustly phosphorylated by PKC δ, but not PKC α, βI, βII, γ, or ϵ, and that the phosphorylation was de-

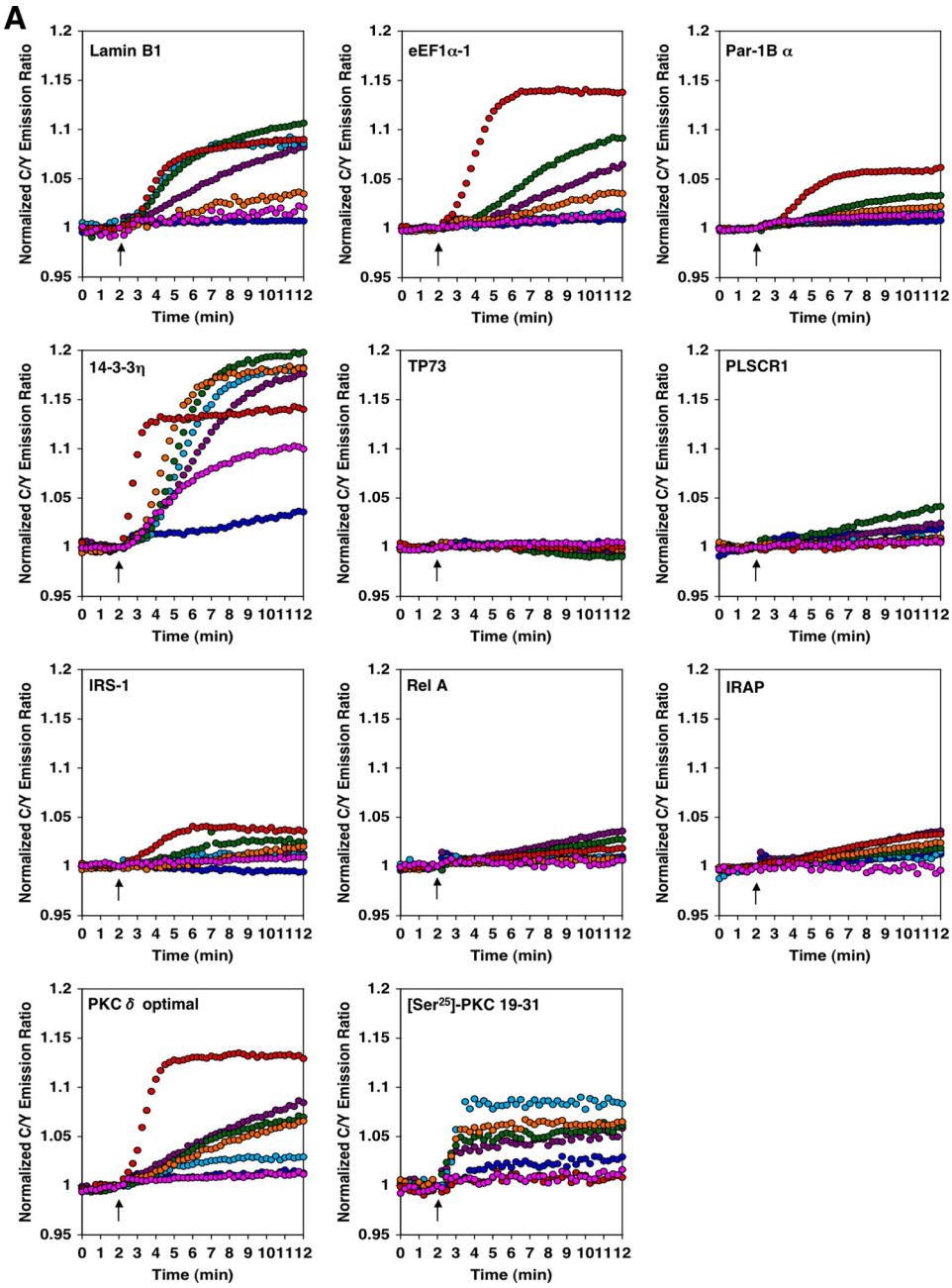

FIGURE 2. **Screening of isotype selectivity of candidate sequences.** *A*, COS7 cells were co-transfected with the candidate constructs of PKC δ-selective CKAR and RFP (*blue*), PKC α-RFP (*purple*), PKC βI-RFP (*cyan*), PKC βII-RFP (*green*), PKC γ-RFP (*orange*), PKC δ-RFP (*red*), or PKC ϵ-RFP (*pink*). The FRET ratio was quantified following the addition of PdBu. The *arrow* indicates the point of PdBu (200 nM) addition. *C/Y*, CFP/YFP. *B*, selectivity of the various constructs for PKC δ was assessed by taking the ratio of the area under the phosphorylation curve (phosphorylation index) obtained using δCKAR to the area obtained using the original CKAR. *Mock* indicates the expression of RFP only.

pendent on phorbol ester-mediated activation. Because Par-1B α is also phosphorylated by PKC ζ (30), we tested whether δCKAR Par-1B α version 12 was phosphorylated by PKC ζ in cells. The Western blot in Fig. 5*D* shows that the reporter was not phosphorylated by PKC ζ, the constitutively active PKM ζ, or the constitutively activated A119E construct of PKC ζ. In contrast, another reporter we have generated, version 1, is phosphorylated by PKM ζ and the A119E mutant of PKC ζ. The above data validate δCKAR Par-1B α version 12 as a highly selective reporter for PKC δ signaling in cells. Henceforth, this reporter will be referred to as δCKAR. Note that while we were optimizing reporters, we used the construct with the eEF1 α sequence (version 2 in Table 2) to study PKC δ activity at a protein scaffold (41); this reporter will be referred to as δCKAR(eEF-1) henceforth. δCKAR is improved because of its higher specificity.

With a reporter for PKC δ, we set out to address the rate, amplitude, and duration of PKC δ activity at various cellular locations. To this end, we targeted the reporter to plasma membrane, Golgi, mitochondria, and nucleus by fusion of appropriate targeting sequences, described previously (21, 23). First, we examined whether the reporter was sensitive

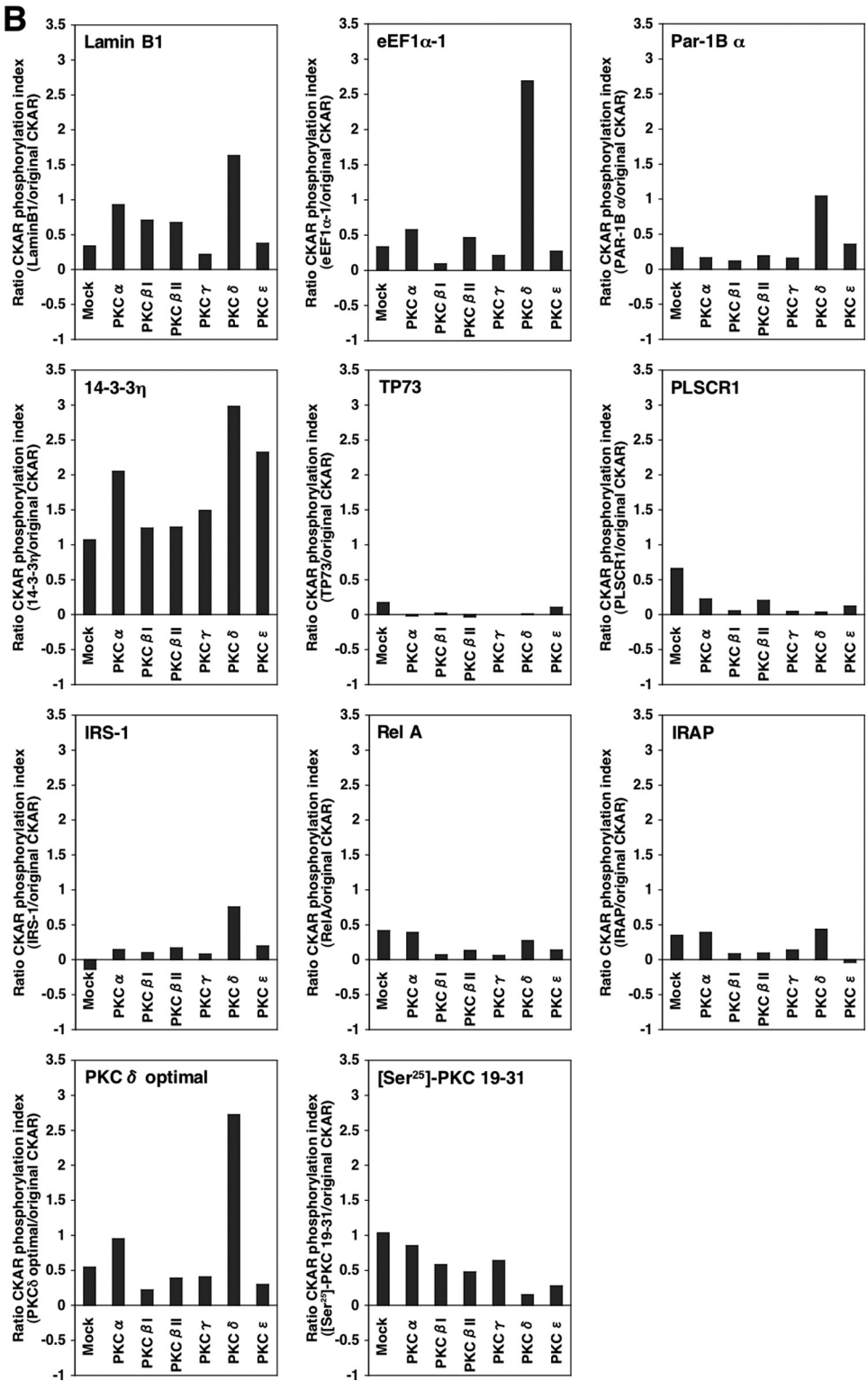

FIGURE 2—*continued*

enough to read out endogenous PKC δ activity. Fig. 6*A* shows that phorbol ester stimulation of COS cells caused a robust increase in endogenous PKC δ activity at the plasma membrane (*red circles*) and a modest increase in activity at Golgi (*green circles*). No activity was detectable in the cytosol (untargeted reporter, *blue circles*), at mitochondria (*orange circles*), or in the nucleus (*pink circles*). To amplify the signal, we overexpressed RFP-tagged PKC δ and examined PKC δ activation in cells expressing comparable levels of kinase (determined by RFP fluorescence). Mirroring the behavior of endogenous PKC δ, the rate and magnitude of activity of overexpressed enzyme were highest at the plasma membrane. The rate of activation at the Golgi was equally fast (half-time of 1 min) but of much lower amplitude. The rate of activation

TABLE 2

Mutations of substrate sequences in candidate PKC δ-selective reporters, Par-1B α, and eEF1α-1

Par-1B α version 1 and eEF1α-1 version 1 are the sequences of candidate reporters Par-1B α and eEF1α-1 as shown in Table. 1, respectively. Bold letters indicate the amino acids mutated from versions 1 and 3 in Par-1B α and versions 1, 2, 4, 5, and 6 in eEF1α- 1. ver., version.

Par-1B α

Version	Position																					
	-9	-8	-7	-6	-5	-4	-3	-2	-1	0	1	2	3	4	5	6	7	8	9	10	11	12
ver.1			R	G	V	S	S	R	S	T	F	H	I	G	Q	L	R	Q	V	R		
ver.2	F	P	R	G	V	S	S	R	S	T	F	H	I	G	Q	L	R	Q	V	R		
ver.3			R	G	V	S	S	R	S	T	F	H	I	G	Q	L	R					
ver.4			**A**	G	V	S	S	R	S	T	F	H	I	G	Q	L	R	Q	V	R		
ver.5			**Q**	G	V	S	S	R	S	T	F	H	I	G	Q	L	R	Q	V	R		
ver.6			R	G	**R**	S	S	R	S	T	F	H	I	G	Q	L	R	Q	V	R		
ver.7			R	G	V	S	S	**Q**	S	T	F	H	I	G	Q	L	R	Q	V	R		
ver.8			R	G	V	S	S	**Q**	S	T	F	H	I	G	Q	L	R					
ver.9			R	G	V	S	S	R	**A**	T	F	H	I	G	Q	L	R	Q	V	R		
ver.10			R	G	V	S	S	R	S	T	**V**	H	I	G	Q	L	R	Q	V	R		
ver.11			R	G	V	S	S	R	S	T	F	**F**	I	G	Q	L	R	Q	V	R		
ver.12			R	G	V	S	S	R	S	T	F	**A**	I	G	Q	L	R	Q	V	R		
ver.13			R	G	V	S	S	R	S	T	F	**G**	I	G	Q	L	R	Q	V	R		
ver.14			R	G	V	S	S	R	S	T	F	**Q**	I	G	Q	L	R	Q	V	R		
ver.15			R	G	V	S	S	R	S	T	F	H	I	G	**G**	L	R	Q	V	R		
ver.16			R	G	V	S	S	R	S	T	F	H	I	G	Q	L	**Q**	Q	V	R		
ver.17			R	G	V	S	S	R	S	T	F	H	I	G	Q	L	R	Q	V	**Q**		
ver.18			**V**	G	**R**	S	S	R	S	T	F	H	I	G	Q	L	R	Q	V	R		
ver.19			R	G	V	**D**	S	R	S	T	F	**A**	I	G	Q	L	R	Q	V	R		
ver.20			R	G	V	**D**	S	R	S	T	F	**Q**	I	G	Q	L	R	Q	V	R		
ver.21			R	G	V	S	S	**Q**	S	T	F	R	I	G	Q	L	R	Q	V	R		
ver.22			R	G	V	S	S	**Q**	S	T	F	R	I	G	Q	L	R					
ver.23			R	G	V	S	S	**Q**	S	T	F	H	I	G	Q	L	R	Q	V	**Q**		
ver.24			R	G	V	S	S	R	S	T	F	**A**	I	G	**G**	L	R	Q	V	R		
ver.25			R	G	V	**A**	**A**	R	**A**	T	F	H	I	G	Q	L	R	Q	V	R		

eEF1α-1

Version	Position																					
	-9	-8	-7	-6	-5	-4	-3	-2	-1	0	1	2	3	4	5	6	7	8	9	10	11	12
ver.1	R	F	A	V	R	D	M	R	Q	T	V	A	I	G	V	I	K	A	V	D	K	K
ver.2		F	A	V	R	D	M	R	Q	T	V	A	I	G	V	I	K	A	V	D	K	K
ver.3	R	F	A	V	R	D	M	R	Q	T	V	A	I	G	V	I	K	A	V	D	K	
ver.4	R	F	A	V	R	D	M	R	Q	T	V	A	I	G	V	I	K	A	V	D		
ver.5		F	A	V	R	D	M	R	Q	T	V	A	I	G	V	I	K	A	V	D		
ver.6				V	R	D	M	R	Q	T	V	A	I	G	V	I	K					
ver.7	R	F	**V**	V	R	D	M	R	Q	T	V	A	I	G	V	I	K	A	V	D		
ver.8	R	F	A	V	**Q**	D	M	R	Q	T	V	A	I	G	V	I	K	A	V	D	K	K
ver.9				V	**Q**	D	M	R	Q	T	V	A	I	G	V	I	K					
ver.10	R	F	A	V	R	**N**	M	R	Q	T	V	A	I	G	V	I	K	A	V	D	K	K
ver.11	R	F	A	V	R	**A**	M	R	Q	T	V	A	I	G	V	I	K	A	V	D	K	K
ver.12	R	F	A	V	R	D	**E**	R	Q	T	V	A	I	G	V	I	K	A	V	D		
ver.13	R	F	A	V	R	D	**Q**	R	Q	T	V	A	I	G	V	I	K	A	V	D		
ver.14	R	F	A	V	R	D	M	**Q**	Q	T	V	A	I	G	V	I	K	A	V	D	K	K
ver.15	R	F	A	V	R	D	M	**K**	Q	T	V	A	I	G	V	I	K	A	V	D		
ver.16	R	F	A	V	R	D	M	R	**A**	T	V	A	I	G	V	I	K	A	V	D	K	K
ver.17	R	F	A	V	R	D	M	R	**E**	T	V	A	I	G	V	I	K	A	V	D		
ver.18	R	F	A	V	R	D	M	R	**S**	T	V	A	I	G	V	I	K	A	V	D		
ver.19	R	F	A	V	R	D	M	R	**G**	T	V	A	I	G	V	I	K	A	V	D		
ver.20	R	F	A	V	R	D	M	R	Q	T	**F**	A	I	G	V	I	K	A	V	D		
ver.21	R	F	A	V	R	D	M	R	Q	T	**D**	A	I	G	V	I	K	A	V	D		
ver.22	R	F	A	V	R	D	M	R	Q	T	V	A	I	G	**G**	I	K	A	V	D	K	K
ver.23	R	F	A	V	R	D	M	R	Q	T	V	A	I	G	V	I	**Q**	A	V	D	K	K
ver.24				V	R	D	M	R	Q	T	V	A	I	G	V	I	**Q**					
ver.25		F	A	V	R	D	M	R	Q	T	V	A	I	G	V	I	K	**D**	V	D	K	K
ver.26	R	F	A	V	R	D	M	R	Q	T	V	A	I	G	V	I	K	A	V	**N**	K	K
ver.27	R	F	A	V	R	D	M	R	Q	T	V	A	I	G	V	I	K	A	V	**A**	K	K
ver.28	R	F	A	V	R	D	M	R	Q	T	V	A	I	G	V	I	K	A	V	**R**		
ver.29	R	F	**R**	V	**A**	D	M	R	Q	T	V	A	I	G	V	I	K	A	V	D	K	K
ver.30	R	F	A	V	R	D	**E**	R	**A**	T	V	A	I	G	**G**	I	K	A	V	**N**		
ver.31		F	A	V	R	D	**E**	R	**A**	T	V	A	I	G	**G**	I	K	A	V	**N**		

of cytosolic PKC δ was considerably slower (half-time of ~4 min) but of comparable amplitude as that at the Golgi. Activity was also detected on the outer membrane of mitochondria; the kinetics of activation were comparable with the cytosolic reporter. No activity was detected in the nucleus. In summary, the maximal agonist-evoked activation of PKC δ occurs at the plasma membrane, followed by Golgi, then cytosol, and then mitochondria.

We next examined the basal PKC δ activity at various cellular locations by measuring the effect of the PKC inhibitor Gö6983 on the base-line FRET ratio of δCKAR. Fig. 6*C* shows that treatment of COS cells with the inhibitor resulted in a decrease in the activity of PKC δ at the plasma membrane (*red circles*), at the Golgi (*green circles*), and at mitochondria (*orange circles*) but did not reduce the activity of either cytosolic or nuclear PKC δ. Thus, basal activity is greatest at the plasma membrane and Golgi, followed by mitochondria.

We also examined the phosphatase suppression at each cellular location by examining how much activity was unveiled by the addition of the phosphatase inhibitor calyculin A. Fig. 6*D* shows that calyculin most effectively unmasked activity at the Golgi (*green circles*) and cytosol (*blue circles*), followed by plasma membrane (*red circles*) and, importantly, nucleus (*pink circles*). No phosphatase suppression was observed at mitochondria. Thus, phosphatases robustly suppress PKC δ activity in the cytosol and Golgi and moderately suppress PKC δ activity in the nucleus and at the plasma membrane. Note that the range of the FRET change at each location differed (unlike that of CKAR, which is constant at all locations except mitochondria (21)), suggesting that phosphatase suppression is not accurately measured using calyculin A as an inhibitor.

We next addressed the ability of natural agonists to activate endogenous PKC δ at various cellular locations (Fig. 7*A*). UTP treatment caused a rapid activation of PKC δ at the plasma membrane (half-time of 1 min) that was relatively robust and decayed with a half-time of ~4 min. Surprisingly, small but reproducible activation of PKC δ was observed in the nucleus (*pink circles*). The kinetics of activation/inactivation were comparable with those observed at the plasma membrane, but the amplitude was significantly smaller. Activation at Golgi was similar in kinetics and magnitude to that in the nucleus. The signature of activation of overexpressed PKC δ was similar to that of endogenous PKC δ, differing only in an ~2-fold increase in magnitude. Specifically, PKC δ activity was greatest at the plasma membrane, followed by nucleus and Golgi. UTP did not cause a detectable increase in PKC δ activity at mitochondria (Fig. 7*B*). The activity at both plasma membrane and Golgi was sustained, with 50% activity still observed 30 min after UTP treatment (Fig. 7*C*).

We further explored the mechanism of activation of PKC δ in the nucleus by monitoring the translocation of RFP-tagged PKC δ into the nucleus. UTP caused PKC δ to translocate into the nucleus (Fig. 8, *A* and *B*) by a mechanism inhibited by the Src inhibitor SU6656. Interestingly, deletion of the C2 domain of PKC δ impaired the agonist-evoked translocation of PKC δ into the nucleus (Fig. 8*B*, *orange circles*). Quantitative analysis of the ratio of RFP-PKC δ in the nucleus when compared with

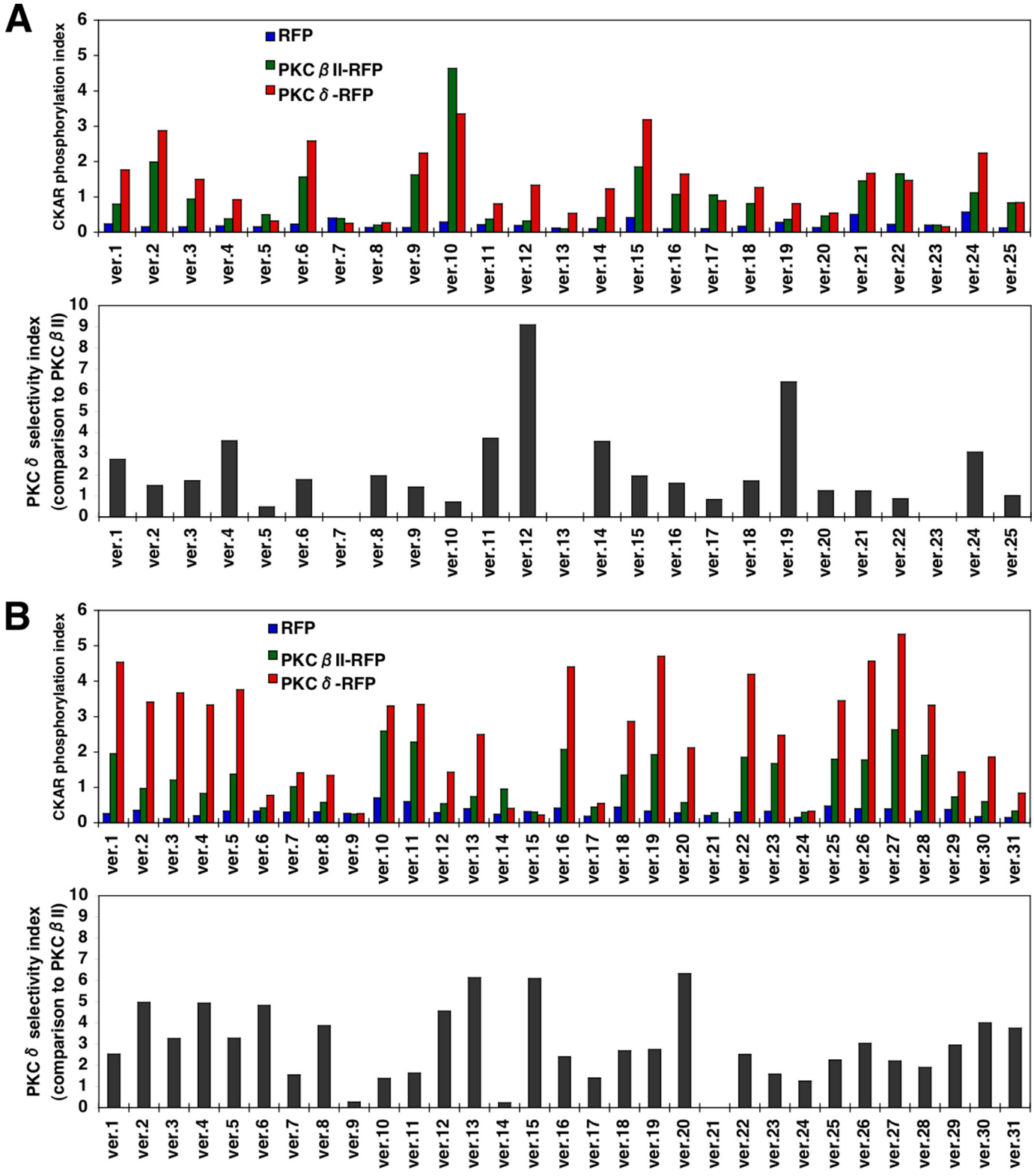

FIGURE 3. **Screen of candidate PKC δ-selective reporters, Par-1B α and eEF1α-1.** *A*, *upper panel*, COS7 cells were co-transfected with δCKAR candidate Par-1B α versions 1–25 (*ver.1–ver.25*) and RFP (*blue*), PKC βII-RFP (*green*), or PKC δ-RFP (*red*). The FRET ratio was quantified following the addition of PdBu (200 nM), and then the CKAR phosphorylation index was calculated as shown under "Experimental Procedures." *Lower panel*, quantification for PKC δ selectivity of candidate reporter Par-1B α versions 1–25 when compared with PKC βII. *B*, *upper panel*, COS7 cells were co-transfected with δCKAR candidate eEF1α-1 versions 1–31 and RFP (*blue*), PKC βII-RFP (*green*), or PKC δ-RFP (*red*). The FRET ratio was quantified following the addition of PdBu (200 nM), and then the CKAR phosphorylation index was calculated as described under "Experimental Procedures." *Lower panel*, quantification for PKC δ selectivity of candidate reporter eEF1α-1 versions 1–31 when compared with PKC βII.

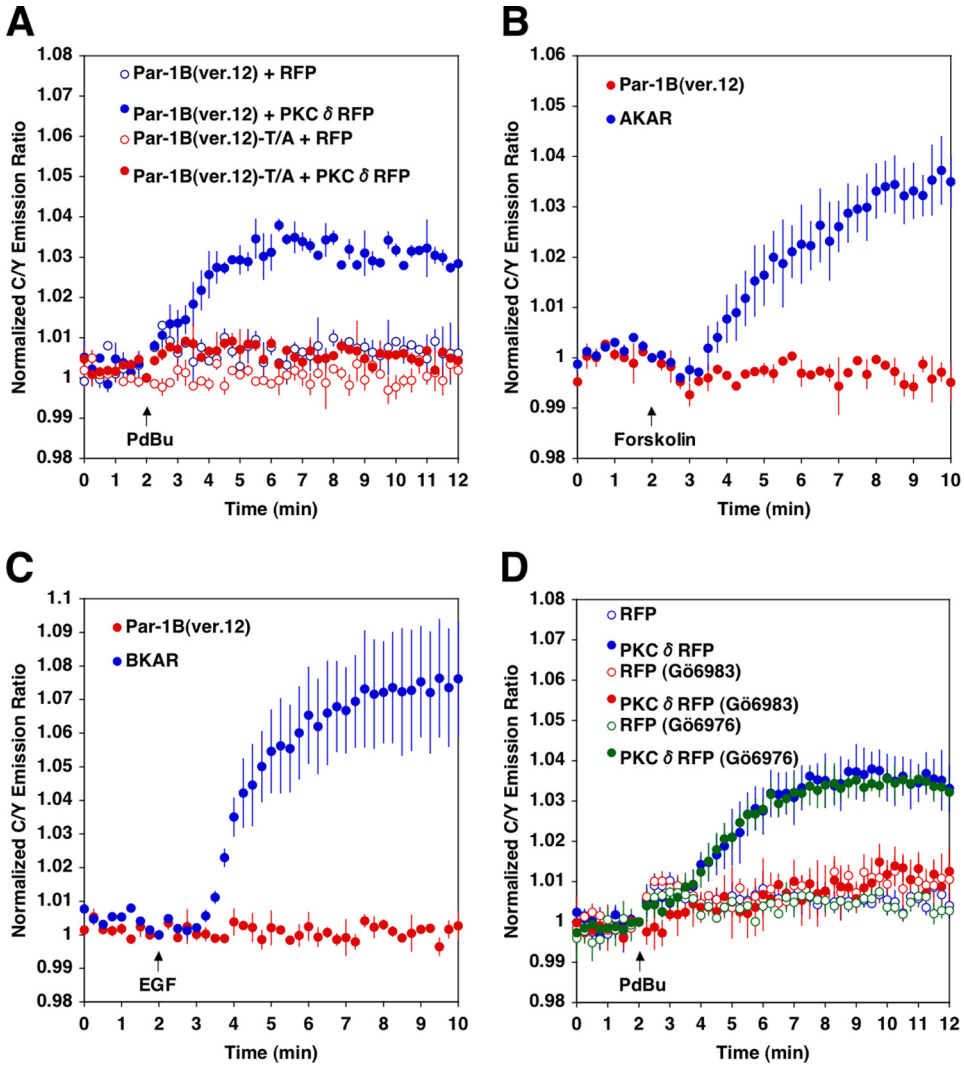

FIGURE 4. **Candidate reporter Par-1B α version 12 is selective to novel PKC.** *A*, COS7 cells were co-transfected with candidate reporter Par-1B α version 12 (*ver.12*, *blue*) or candidate reporter Par-1B α version 12-T/A (*red*) and RFP (*open circle*) or PKC δ-RFP (*closed circle*). The FRET ratio was quantified following the addition of PdBu (200 nM). *C/Y*, CFP/YFP. *B*, COS7 cells were transfected with candidate reporter Par-1B α version 12 (*red*) or AKAR (*blue*). The FRET ratio was quantified following the addition of forskolin (10 μM). *C*, COS7 cells were co-transfected with candidate reporter Par-1B α version 12 (*red*) or BKAR (*blue*) and PKB-RFP. The FRET ratio was quantified following the addition of EGF (50 ng/ml). *D*, COS7 cells co-transfected with candidate reporter Par-1B α version 12 and RFP (*open circles*) or PKC δ-RFP (*closed circles*) were treated with DMSO vehicle (*blue*), Gö6983 (*red*), or Gö6976 (*green*) for 30 min. At this point, the FRET ratio was measured before and after the addition of PdBu (200 nM). Data represent the average ± S.E. from at least three independent experiments.

that in the cytosol for cells overexpressing PKC δ or the construct lacking the C2 domain, before or after treatment with UTP, and with or without pretreatment with SU6656, confirmed that UTP increased the amount of PKC δ in the nucleus, that this increase was abolished in cells treated with the Src inhibitor, and that deletion of the C2 domain caused slightly more accumulation of PKC δ in the nucleus, but this construct of PKC was insensitive to UTP (Fig. 8*C*). Note that nuclear targeting of a diacylglycerol reporter (21) revealed no changes in nuclear diacylglycerol following UTP stimulation of cells (data not shown).

The sensitivity of translocation of PKC δ into the nucleus to the Src inhibitor led us to ask whether nuclear activity was also sensitive to Src inhibition. Fig. 8*D* shows that the UTP-induced activation of PKC δ in the nucleus (read-out by nuclear-localized δCKAR) was suppressed by SU6656 to basal levels (*i.e.* that observed in cells not overexpressing PKC δ). Similar data were obtained for endogenous PKC δ (Fig. 8*E*). Similarly, deletion of the C2 domain abolished the ability of UTP to increase PKC δ activity in the nucleus (Fig. 8*D*). These data reveal that the activation of PKC δ in the nucleus depends on Src kinase activity and the C2 domain of PKC δ.

Because Src controls the translocation of PKC δ into the nucleus, we next asked whether PKC δ already present in the nucleus is sensitive to Src inhibition. To this end, we monitored the UTP-dependent activation of nuclear-targeted PKC δ using nuclear-targeted δCKAR. Fusion of an NLS onto the C terminus of the C-terminally RFP-tagged PKC δ results in constitutive sequestration in the nucleus (supplemental Fig. 1), as reported previously by Reyland and co-workers (4) for GFP-tagged PKC δ with an additional NLS. Fig. 9*A* shows that the activity of PKC δ already sequestered in the nucleus was inhibited by SU6656 (*pink circles*). To validate the specificity of the inhibition, we compared the effects of the Src inhibitor

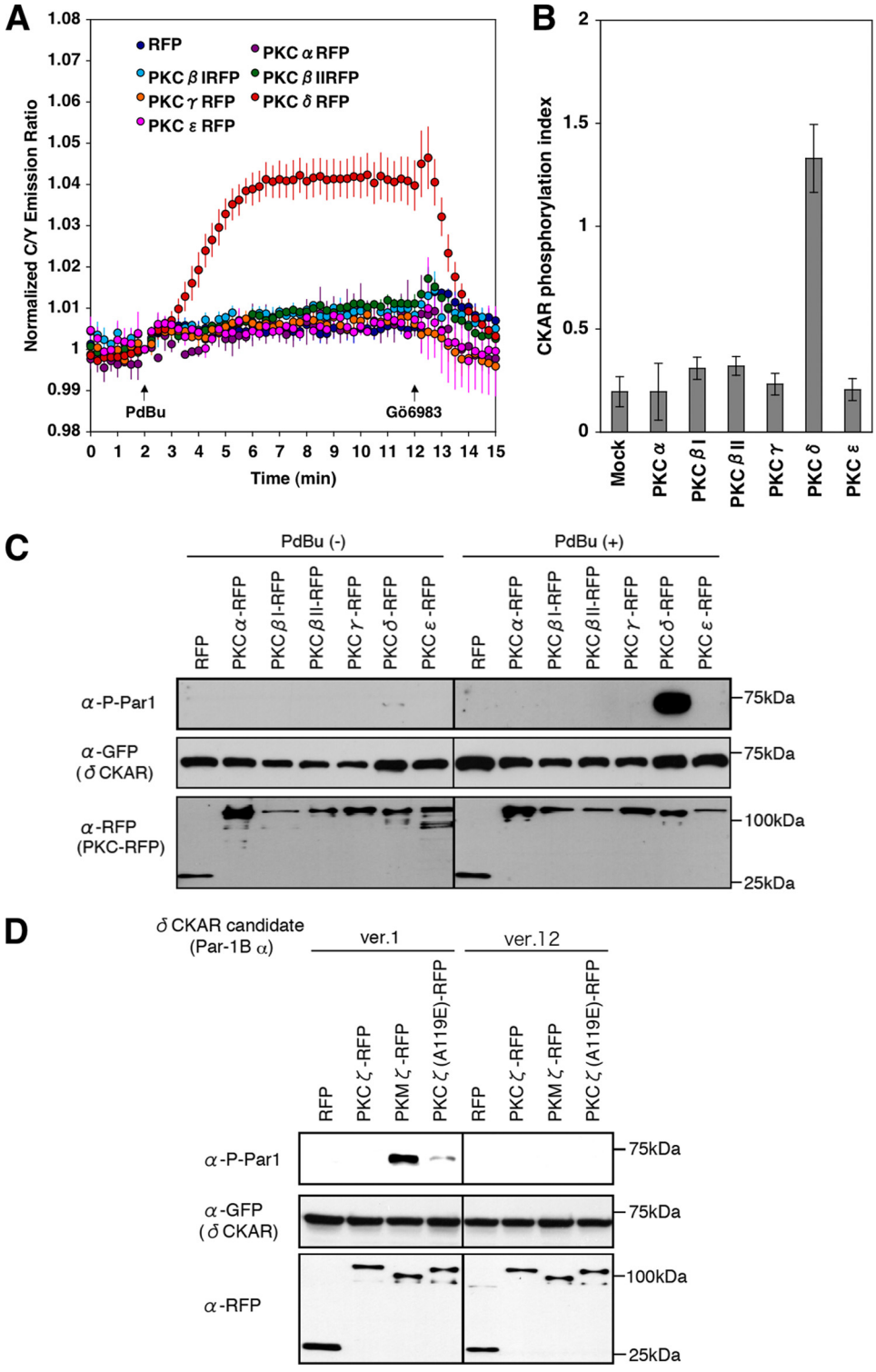

FIGURE 5. **Candidate reporter Par-1B α version 12 is selective for PKC δ.** *A*, COS7 cells were co-transfected with δCKAR candidate Par-1B α version 12 and RFP, PKC α-RFP, PKC βI-RFP, PKC βII-RFP, PKC γ-RFP, PKC δ-RFP, or PKC ε-RFP. The FRET ratio was quantified following the addition of PdBu (200 nM) and then the PKC inhibitor Gö6983 (500 nM). Data represent the average ± S.E. from at least three independent experiments. *C/Y*, CFP/YFP. *B*, quantification of candidate reporter Par-1B α version 12 phosphorylation. The CKAR phosphorylation index was calculated from the result of Fig. 4*A*. *Mock* indicates the expression of RFP only. *C*, COS7 cells were co-transfected with δCKAR candidate Par-1B α version 12 and RFP, PKC α-RFP, PKC βI-RFP, PKC βII-RFP, PKC γ-RFP, PKC δ-RFP, or PKC ε-RFP. Phosphorylation of Par-1B α version 12 was detected before or after stimulation with PdBu (200 nM) using anti-phospho-Par-1 (α-*P-Par1*) antibody. Immunoblot of the δCKAR candidate Par-1B α version 12 or PKC-RFP was detected using anti-GFP antibody (α-*GFP*) or anti-RFP antibody (α-*RFP*), respectively. *D*, COS7 cells were co-transfected with δCKAR candidate Par-1B α version 1 (*ver.1*) or version 12 and RFP, PKC ζ-RFP, PKM ζ-RFP, or PKC ζ(A119E)-RFP. Phosphorylation of these reporters was detected at 24 h after the transfection using anti-phospho-Par-1 (α-*P-Par1*) antibody. Immunoblot of the reporters or PKC-RFP was performed using anti-GFP antibody (α-*GFP*) or anti-RFP antibody (α-*RFP*), respectively.

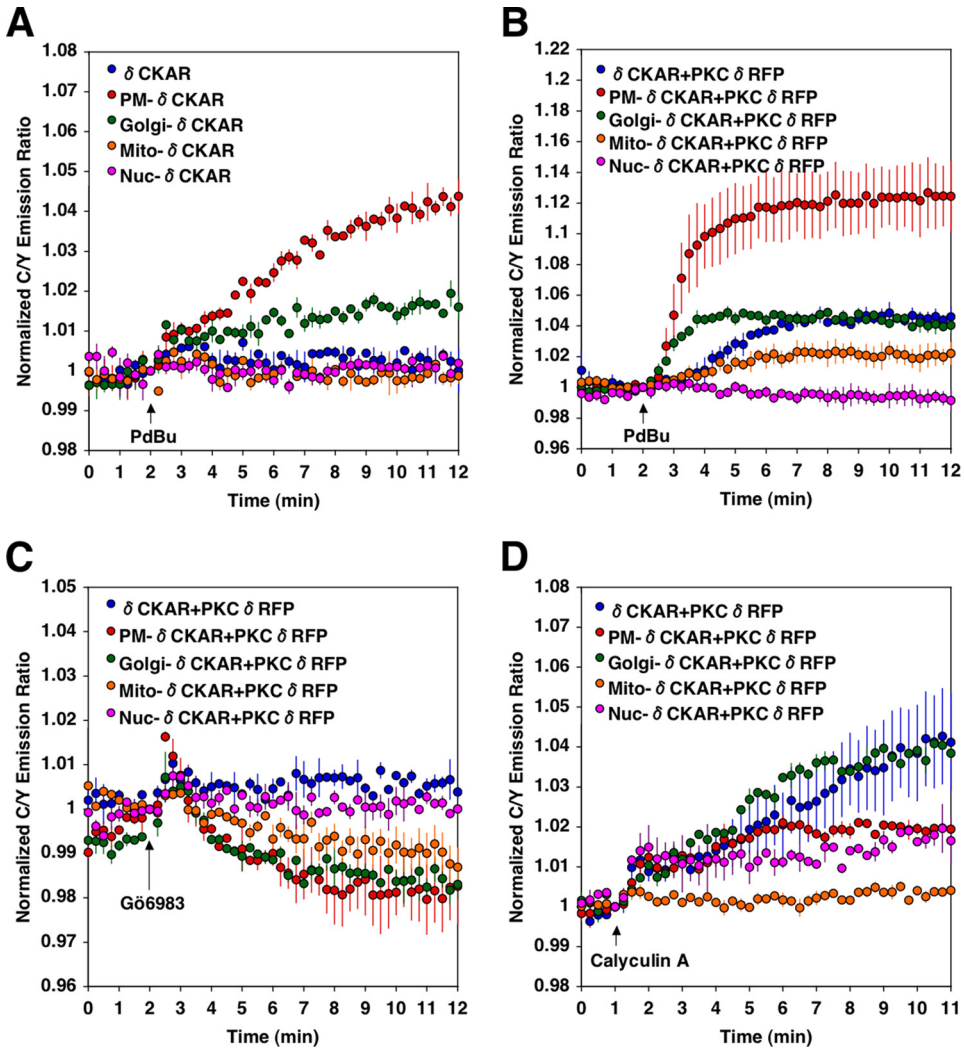

FIGURE 6. **Spatiotemporal dynamics of PKC δ activity induced by PdBu in COS7 cells.** *A*, COS7 cells were transfected with the indicated targeted constructs of δCKAR, and the CFP/YFP (*C/Y*) emission ratio was quantified as a function of time following PdBu (200 nM) treatment: δCKAR (*blue*), PM-δCKAR (*red*), Golgi-δCKAR (*green*), Mito-δCKAR (*orange*), and Nuc-δCKAR (*pink*). *B*, COS7 cells were co-transfected with the indicated targeted constructs of δCKAR and PKC δ-RFP, and the CFP/YFP emission ratio was quantified as a function of time following PdBu (200 nM) treatment: δCKAR (*blue*), PM-δCKAR (*red*), Golgi-δCKAR (*green*), Mito-δCKAR (*orange*), and Nuc-δCKAR (*pink*). These data reveal the magnitude of the phorbol ester-stimulated response. *C*, COS7 cells were co-transfected with targeted δCKAR constructs and PKC δ-RFP. The FRET ratio was monitored following treatment with Gö6983 (500 nM), an inhibitor of conventional and novel PKC isozymes. These data reveal the magnitude of the basal conventional PKC activity at each location. *D*, COS7 cells co-transfected with various targeted δCKAR constructs and PKC δ-RFP were stimulated with PdBu (200 nM) for 20 min until the maximal phorbol ester stimulation was achieved. At this point, the FRET ratio was measured before and after the addition of calyculin A (100 μM) to inhibit cellular phosphatases. The magnitude of the calyculin A-stimulated response reveals the phosphatase-suppressed PKC activity at each region. Data represent the average ± S.E. from at least three independent experiments.

PP2 and its non-inhibiting counterpart PP3; the active inhibitor PP2 suppressed the activity of nuclear PKC δ (*yellow circles*), whereas the inactive control compound, PP3, had no effect (*green circles*). The Src dependence for activation was specific for PKC δ in the nucleus; neither plasma membrane- (Fig. 9*B*) nor Golgi- (Fig. 9*C*) tethered δCKAR was affected by the Src inhibitors. These data establish that Src is required for PKC δ in the nucleus to be activated.

DISCUSSION

We have developed an activity reporter for PKC δ that allows measurement of the spatiotemporal dynamics of this isozyme, specifically, in lipid second messenger signaling in live cells. We show that PKC δ is most active at the plasma membrane, both basally and following agonist stimulation, with limited activity at Golgi and at the mitochondrial outer membrane. Additionally, we show that the nucleus serves as a hub for PKC δ signaling following treatment of cells with a G-protein-coupled receptor agonist, UTP, but not phorbol esters. This nuclear activation depends on the activity of Src family kinases, which control not only the entry of PKC δ into the nucleus, as established previously (1) but, additionally, the catalytic activity of PKC δ in the nucleus. Thus, PKC δ signals by two distinct mechanisms following agonist stimulation: 1) signaling that depends only on the presence of a C1 ligand (diacylglycerol or phorbol esters) and that is primarily at the plasma membrane but also at the Golgi and mitochondrial surface and 2) signaling that requires Tyr phosphorylation and that is constrained to the nucleus.

CKAR and δCKAR—The first generation reporter for PKC activity, CKAR, was designed to measure bulk PKC activity in cells (20, 42). Here we show that, indeed, CKAR faithfully

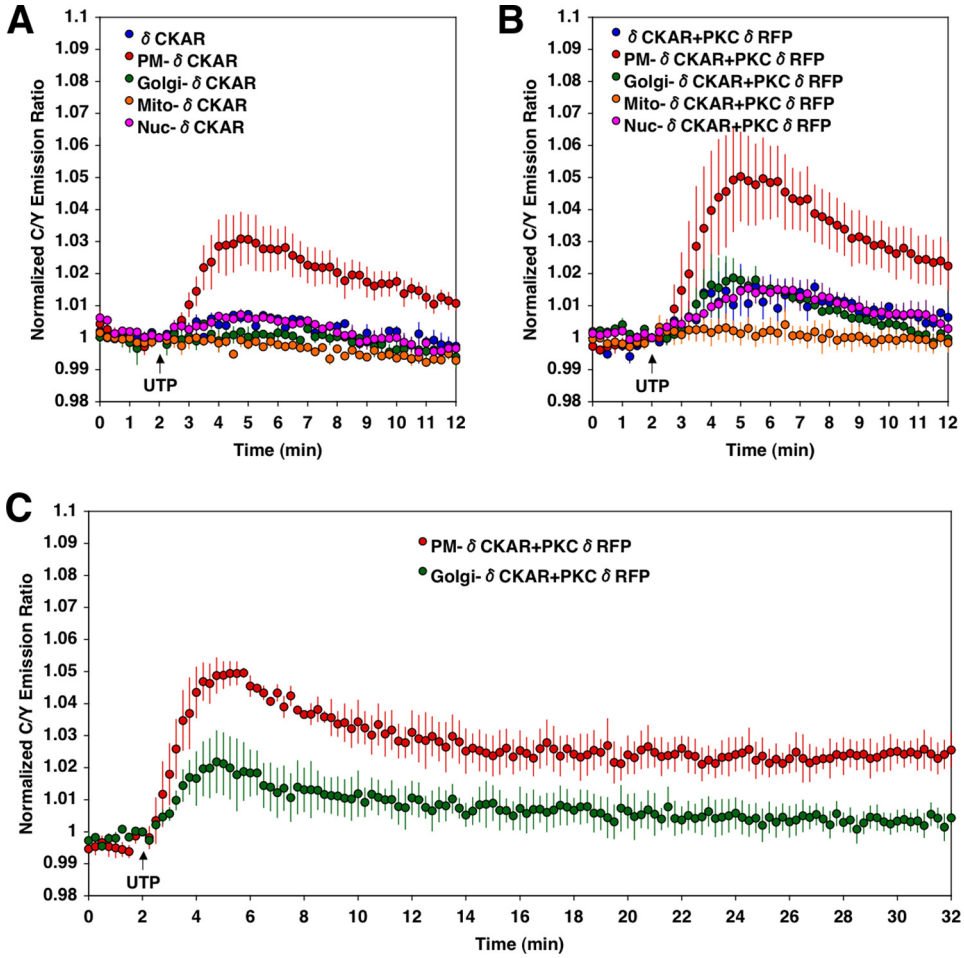

FIGURE 7. **Spatiotemporal dynamics of PKC δ activity induced by UTP in HeLa cells.** *A*, HeLa cells were transfected with the indicated targeted constructs of δCKAR, and the CFP/YFP (*C/Y*) emission ratio was quantified as a function of time following UTP (100 μM) treatment: δCKAR (*blue*), PM-δCKAR (*red*), Golgi-δCKAR (*green*), Mito-δCKAR (*orange*), and Nuc-δCKAR (*pink*). *B*, HeLa cells were co-transfected with the indicated targeted constructs of δCKAR and PKC δ-RFP, and the CFP/YFP emission ratio was quantified as a function of time following UTP (100 μM) treatment: δCKAR (*blue*), PM-δCKAR (*red*), Golgi-δCKAR (*green*), Mito-δCKAR (*orange*), and Nuc-δCKAR (*pink*). *C*, HeLa cells were co-transfected with PM-δCKAR (*red*) or Golgi-δCKAR (*green*) and PKC δ-RFP, and the CFP/YFP emission ratio was quantified to 30 min as a function of time following UTP (100 μM) treatment. Data represent the average ± S.E. from at least three independent experiments.

reads out the activity of conventional and novel PKC family members without significant discrimination among isozymes. Specifically, overexpression of conventional (PKC α, βI, βII, γ) or novel (PKC δ, ϵ) isozymes in COS7 cells revealed that the rate of phorbol ester-stimulated phosphorylation of CKAR was comparable for all isozymes, with half-times for maximal phosphorylation ranging from 0.5 (PKC βII) to 1.5 min (PKC δ). Interestingly, the magnitude of the response differed for the various isozymes. Because the dynamic range of the reporter would be the same regardless of the isozyme co-expressed in cells, the magnitude serves as a measure of the basal activity of each of these kinases. Thus, the basal activity of the isozymes ranks PKC ϵ > PKC α/δ > PKC βI/βII/γ. Consistent with this ranking, the addition of the PKC inhibitor Gö6983 reversed activity to considerably below base line for PKC ϵ and PKC α and reversed activity to base-line levels for the other isozymes. Thus, previous studies using CKAR present an average of the contribution of conventional and novel isozymes, which are all effectively read out by the reporter.

Replacement of the phosphorylation sequence of CKAR with that of 11 sequences previously identified as selective for PKC δ allowed us to identify a sequence that was phosphorylated by PKC δ and functional in a reporter that uses FHA2 as the phospho-peptide binding module (23). Optimization of this sequence resulted in a new version of CKAR, δCKAR, that is highly selective for PKC δ over all other isozymes tested. Importantly, the reporter selectively reads out the activity of PKC δ when compared with other PKC isozymes and is not a substrate for the related basophilic kinases Akt/PKB and PKA.

Targeted δCKAR—We have previously shown that G-protein-coupled receptor agonists cause rapid activation of conventional PKC isozymes primarily at the plasma membrane, an event driven by a rapid spike in Ca^{2+}; this is followed by slower activation of novel PKC isozymes primarily at Golgi that is driven by diacylglycerol. Activity at both membrane locations is sustained by the persistence of diacylglycerol. Taken together, the net PKC activity is highest at the Golgi, followed by plasma membrane. Here we show that, surpris-

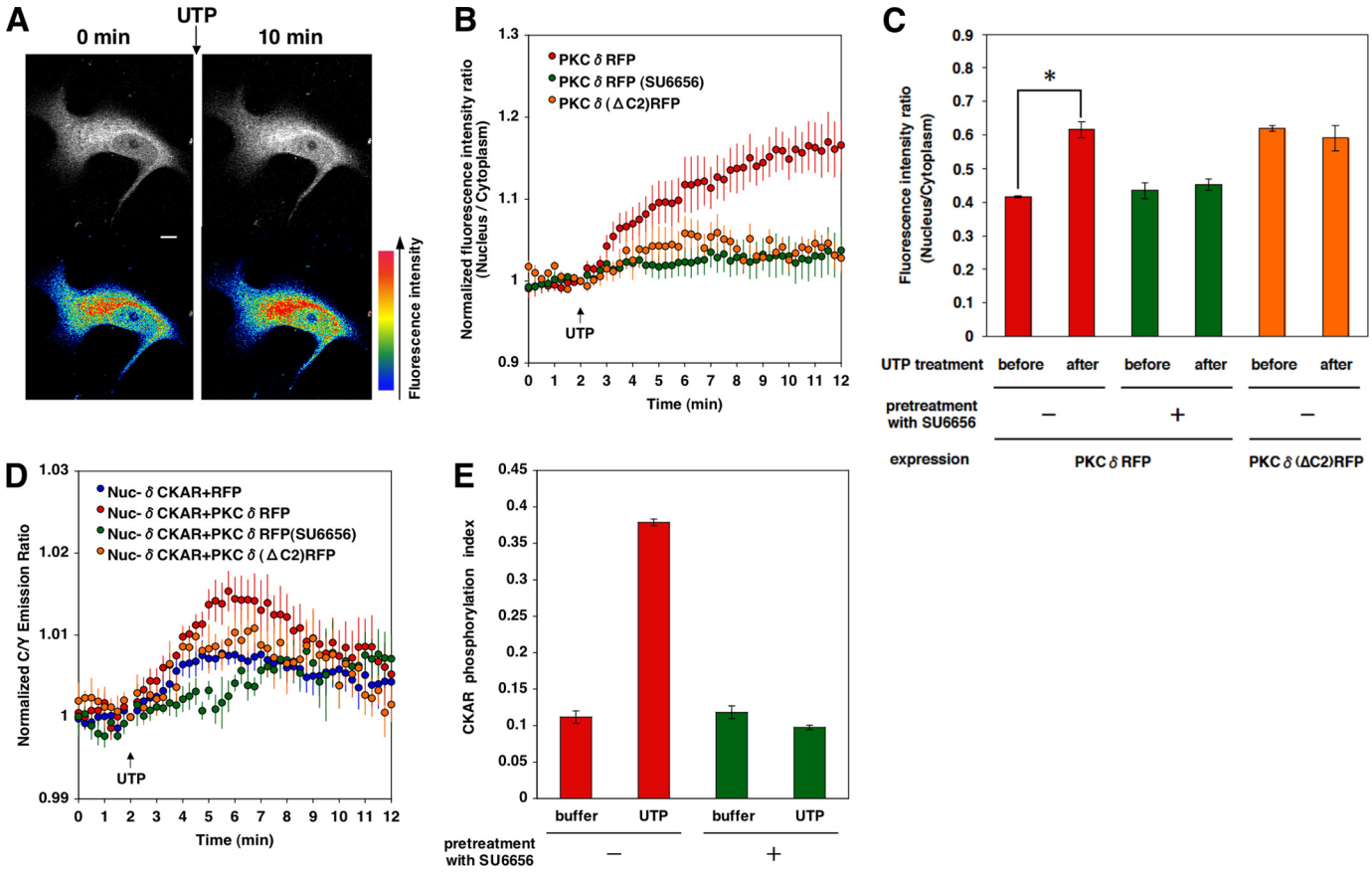

FIGURE 8. **UTP induces nuclear translocation and activation of PKC δ, effects mediated by Src family tyrosine kinases.** *A*, HeLa cells were transfected with the PKC δ-RFP, and the fluorescence intensity of RFP was detected before and after UTP (100 μM) stimulation using confocal laser scanning microscopy. Pseudo-color images were analyzed by the LSM 510 META software. *Bar*, 10 μm. *B*, HeLa cells were transfected with the PKC δ-RFP or C2-deleted PKC δ-RFP (*PKC δ(ΔC2)RFP*). Cells were then pretreated with DMSO vehicle or 2 μM SU6656, a selective Src family kinase inhibitor, for 30 min and then stimulated with UTP (100 μM). The fluorescence intensity of RFP was detected using confocal laser scanning microscopy. Then the fluorescence intensity ratio (*Nucleus/Cytoplasm*) was quantified as a function of time following UTP treatment. *C*, HeLa cells were transfected with the PKC δ-RFP or C2-deleted PKC δ-RFP (*PKC δ(ΔC2)RFP*). Cells were then pretreated with DMSO vehicle or 2 μM SU6656, a selective Src family kinase inhibitor, for 30 min and then stimulated with UTP (100 μM). Cells were fixed at the point of 0 or 10 min after UTP stimulation. The fluorescence intensity of RFP was detected using confocal laser scanning microscopy. Then the fluorescence intensity ratio (*Nucleus/Cytoplasm*) was quantified. *, $p < 0.05$ (Student's *t* test) *D*, HeLa cells were co-transfected with the Nuc-δCKAR and RFP, PKC δ-RFP or C2-deleted PKC δ-RFP (*PKC δ(ΔC2)RFP*). Cells were then pretreated with DMSO vehicle or 2 μM SU6656 for 30 min and then stimulated with UTP (100 μM). The CFP/YFP (*C/Y*) emission ratio was quantified as a function of time following UTP (100 μM) treatment. Data represent the average ± S.E. from at least three independent experiments. *E*, HeLa cells were transfected with Nuc-δCKAR. Cells were then pretreated with DMSO vehicle or 2 μM SU6656 for 30 min and then stimulated with buffer control or UTP (100 μM). The CFP/YFP emission ratio was quantified for 10 min following UTP (100 μM) treatment, and the CKAR phosphorylation index was calculated as described under "Experimental Procedures."

ingly, the novel PKC isozyme PKC δ is considerably more active at plasma membrane than Golgi. Its activation kinetics at both membrane locations mirror those for the production of diacylglycerol (see Ref. 21), with a half-time of approximately 1 min. Phosphatase suppression of δCKAR phosphorylation is relatively modest at the plasma membrane, consistent with findings using CKAR that there is very little phosphatase suppression of net PKC activity at the plasma membrane. In contrast, PKC δ activity at Golgi and in the cytosol is strongly opposed by phosphatases, whereas bulk PKC activity is really only strongly suppressed by phosphatases in the cytosol and nucleus. Basal activity of PKC δ is highest at the plasma membrane, consistent with the read-out from CKAR that net PKC activity has high basal levels at this location. In addition, we found some agonist-evoked activity of PKC δ at the outer membrane of mitochondria. This supports several reports showing that PKC δ phosphorylates mitochondrial proteins (6, 43–45). Taken together, these data reveal that the plasma membrane is the primary site of action not only of Ca^{2+}-regulated PKC isozymes but also of the novel isozyme PKC δ.

The Nucleus as a Hub of PKC δ Activity—PKC δ is a pro-apoptotic kinase (1, 3), exerting many of its biological functions in the nucleus. However, there is no evidence to date that this isozyme signals in the nucleus in the absence of apoptotic stimuli. Here we show that G-protein-coupled receptor agonists effectively activate PKC δ in the nucleus. This activation is not triggered by phorbol esters, which cause robust activation of PKC δ at non-nuclear locations such as plasma membrane, Golgi, and mitochondria. Rather, nuclear activity depends on activation of Src family kinases. Reyland and coworkers (5) have previously shown that PKC δ has an NLS that becomes unmasked following Tyr phosphorylation at Tyr^{64} in the C2 domain and Tyr^{155} in the C1 domain. These phosphorylations are required for the nuclear translocation triggered by apoptotic stimuli and are catalyzed by Src family kinases. Here we show that the UTP-mediated translocation

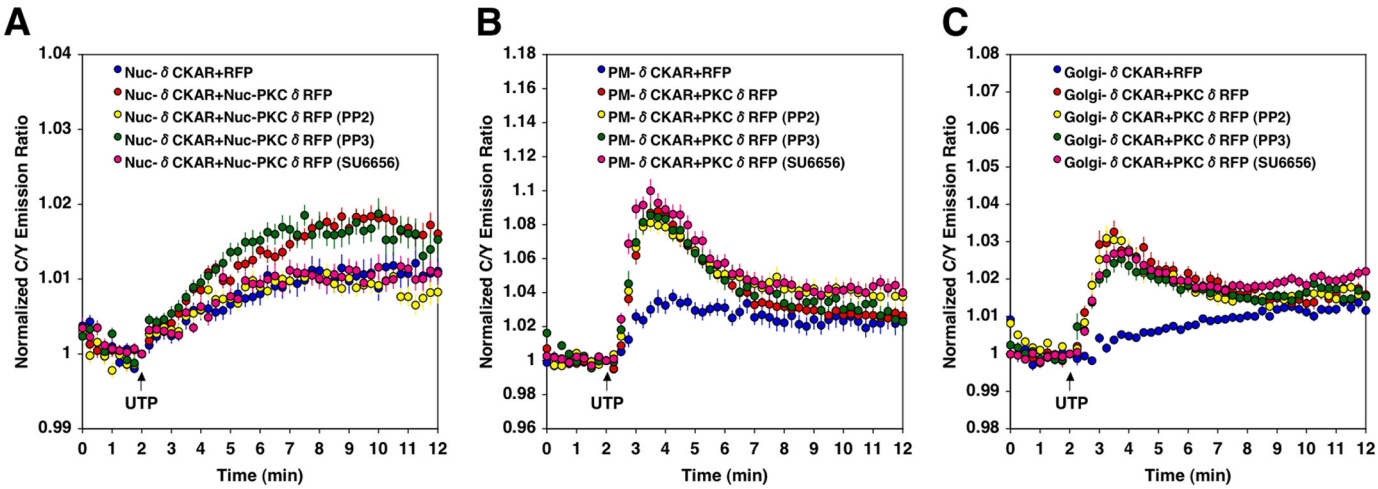

FIGURE 9. **UTP induces activation of PKC δ in nucleus that depends on activity of Src family tyrosine kinase.** *A*, HeLa cells were co-transfected with the Nuc-δCKAR and RFP or Nuc-PKC δ-RFP. Cells were then pretreated with DMSO vehicle, 10 μM PP2, 10 μM PP3, or 2 μM SU6656 for 30 min and then stimulated with UTP (100 μM). The CFP/YFP (*C/Y*) emission ratio was quantified as a function of time following UTP (100 μM) treatment. *B*, HeLa cells were co-transfected with PM-δCKAR and RFP or PKC δ-RFP. Cells were then pretreated with DMSO vehicle, 10 μM PP2, 10 μM PP3, or 2 μM SU6656 for 30 min and then stimulated with UTP (100 μM). The CFP/YFP emission ratio was quantified as a function of time following UTP (100 μM) treatment. *C*, HeLa cells were co-transfected with Golgi-δCKAR and RFP or PKC δ-RFP. Cells were then pretreated with DMSO vehicle, 10 μM PP2, 10 μM PP3, 2 μM SU6656 for 30 min and then stimulated with UTP (100 μM). The CFP/YFP emission ratio was quantified as a function of time following UTP (100 μM) treatment. Data represent the average ± S.E. from at least three independent experiments.

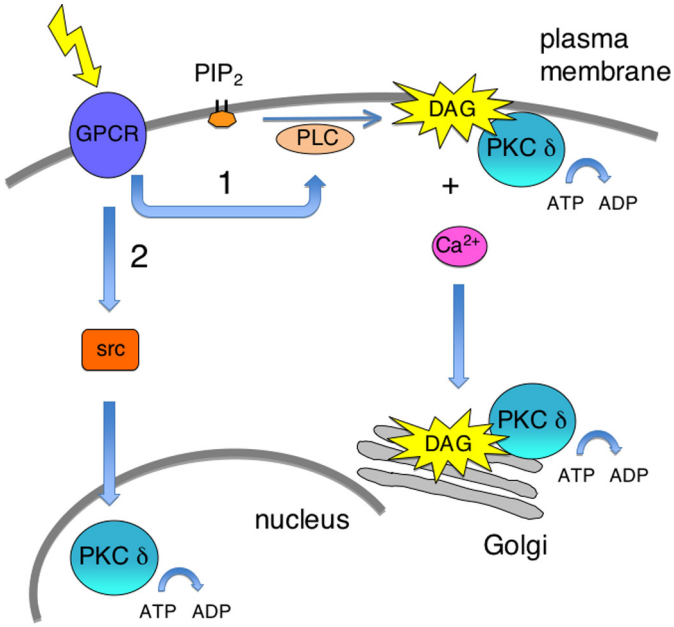

FIGURE 10. **Model showing two mechanisms of activation of PKC δ.** Stimulation of cells with UTP causes the activation of PKC δ by the canonical phospholipase C (*PLC*)-mediated hydrolysis of phosphatidylinositol 4,5-bisphosphate (*PIP_2*) to generate diacylglycerol (*DAG*) in the plasma membrane and Golgi (***1***) and activation of Src, which in turn activates PKC δ in the nucleus (***2***). The active species of PKC δ is denoted by the hydrolysis of ATP. Note that we have previously shown that stimuli received at the cell surface use Ca^{2+} as the mediator to elevate diacylglycerol levels at the Golgi (50). In the first mechanism, diacylglycerol directly binds and activates PKC δ at the plasma membrane, primarily, and at the Golgi, to a lesser extent. This ligand-dependent activity is insensitive to Src and can be fully induced by phorbol esters. In the second mechanism, the activity of Src is necessary for the activation of PKC δ in the nucleus; this activity cannot be induced by phorbol esters. *GPCR*, G-protein-coupled receptor.

of PKC δ into the nucleus is also prevented by Src inhibitors. However, in addition, the activity of PKC δ that is already in the nucleus depends on Src kinases; UTP causes activation of PKC δ that is sequestered in the nucleus by an additional NLS sequence, and this activation is prevented by two different Src inhibitors, PP2 and SU6656, but not the inactive PP3. These data reveal that PKC δ is activated in the nucleus following G-protein-coupled receptor agonist-triggered signaling, revealing that its nuclear activation is not restricted to apoptotic stimuli. Note that phorbol esters effectively activate other PKC isozymes in the nucleus, although this activity is only unveiled in the presence of phosphatase inhibitors (21).

Our data support a model in which PKC δ signals by two mechanisms: a Src kinase-independent mechanism at non-nuclear locations that can be initiated by phorbol esters/diacylglycerol and a Src kinase-dependent mechanism in the nucleus that cannot be activated by phorbol esters (Fig. 10). The ability of UTP to stimulate nuclear activity suggests that P2Y receptors couple to Src kinase. Indeed, P2Y receptors have a P*XX*P motif that binds the SH3 domain of Src, an event that activates the kinase (46). Consistent with activation of Src by P2Y receptors, the ability of P2Y receptors to activate the MAP kinase pathway is prevented by inhibition of Src (47–49). Our data are consistent with UTP activating two pathways that differentially control PKC δ: 1) phospholipase C-mediated hydrolysis of phosphoinositides to generate diacylglycerol, which activates PKC δ at intracellular membranes by a mechanism independent of Tyr phosphorylation, and 2). Src-mediated activation of PKC δ in the nucleus. The mechanism by which nuclear PKC δ is activated by Src remains to be resolved, but the inability of phorbol esters to activate PKC δ in the nucleus suggests that modification of either the PKC or a binding partner is essential for catalytic activity in this compartment.

Acknowledgments—We thank Maya Kunkel for suggestions and critical reading of the manuscript, Lisa Gallegos for helpful discussions, and Alyssa Wu for technical assistance.

REFERENCES

1. Reyland, M. E. (2007) *Biochem. Soc. Trans.* **35,** 1001–1004
2. Griner, E. M., and Kazanietz, M. G. (2007) *Nat. Rev. Cancer* **7,** 281–294
3. Brodie, C., and Blumberg, P. M. (2003) *Apoptosis* **8,** 19–27
4. DeVries-Seimon, T. A., Ohm, A. M., Humphries, M. J., and Reyland, M. E. (2007) *J. Biol. Chem.* **282,** 22307–22314
5. Humphries, M. J., Ohm, A. M., Schaack, J., Adwan, T. S., and Reyland, M. E. (2008) *Oncogene* **27,** 3045–3053
6. Majumder, P. K., Pandey, P., Sun, X., Cheng, K., Datta, R., Saxena, S., Kharbanda, S., and Kufe, D. (2000) *J. Biol. Chem.* **275,** 21793–21796
7. Gonzalez-Guerrico, A. M., and Kazanietz, M. G. (2005) *J. Biol. Chem.* **280,** 38982–38991
8. Kajimoto, T., Ohmori, S., Shirai, Y., Sakai, N., and Saito, N. (2001) *Mol. Cell. Biol.* **21,** 1769–1783
9. Kajimoto, T., Shirai, Y., Sakai, N., Yamamoto, T., Matsuzaki, H., Kikkawa, U., and Saito, N. (2004) *J. Biol. Chem.* **279,** 12668–12676
10. Blass, M., Kronfeld, I., Kazimirsky, G., Blumberg, P. M., and Brodie, C. (2002) *Mol. Cell. Biol.* **22,** 182–195
11. Reyland, M. E., Barzen, K. A., Anderson, S. M., Quissell, D. O., and Matassa, A. A. (2000) *Cell Death Differ* **7,** 1200–1209
12. Tanaka, Y., Gavrielides, M. V., Mitsuuchi, Y., Fujii, T., and Kazanietz, M. G. (2003) *J. Biol. Chem.* **278,** 33753–33762
13. von Burstin, V. A., Xiao, L., and Kazanietz, M. G. (2010) *Mol Pharmacol* **78,** 325–332
14. Nishizuka, Y. (1992) *Science* **258,** 607–614
15. Newton, A. C. (2010) *Am. J. Physiol. Endocrinol. Metab.* **298,** E395–402
16. Newton, A. C. (2009) *J. Lipid Res.* **50,** (suppl.) S266–S271
17. Dries, D. R., Gallegos, L. L., and Newton, A. C. (2007) *J. Biol. Chem.* **282,** 826–830
18. Carrasco, S., and Merida, I. (2004) *Mol. Biol. Cell* **15,** 2932–2942
19. Schechtman, D., and Mochly-Rosen, D. (2001) *Oncogene* **20,** 6339–6347
20. Violin, J. D., Zhang, J., Tsien, R. Y., and Newton, A. C. (2003) *J. Cell Biol.* **161,** 899–909
21. Gallegos, L. L., Kunkel, M. T., and Newton, A. C. (2006) *J. Biol. Chem.* **281,** 30947–30956
22. Gallegos, L. L., and Newton, A. C. (2008) *IUBMB Life* **60,** 782–789
23. Kunkel, M. T., and Newton, A. C. (2010) *Curr. Prot. Chem. Biol.* **1,** 17–28
24. Zhang, J., Hupfeld, C. J., Taylor, S. S., Olefsky, J. M., and Tsien, R. Y. (2005) *Nature* **437,** 569–573
25. Zhang, J., Ma, Y., Taylor, S. S., and Tsien, R. Y. (2001) *Proc. Natl. Acad. Sci. U.S.A.* **98,** 14997–15002
26. Kunkel, M. T., Ni, Q., Tsien, R. Y., Zhang, J., and Newton, A. C. (2005) *J. Biol. Chem.* **280,** 5581–5587
27. Giorgione, J. R., Lin, J. H., McCammon, J. A., and Newton, A. C. (2006) *J. Biol. Chem.* **281,** 1660–1669
28. Murray, N. R., Burns, D. J., and Fields, A. P. (1994) *J. Biol. Chem.* **269,** 21385–21390
29. Kielbassa, K., Müller, H. J., Meyer, H. E., Marks, F., and Gschwendt, M. (1995) *J. Biol. Chem.* **270,** 6156–6162
30. Hurov, J. B., Watkins, J. L., and Piwnica-Worms, H. (2004) *Curr. Biol.* **14,** 736–741
31. Suzuki, A., Hirata, M., Kamimura, K., Maniwa, R., Yamanaka, T., Mizuno, K., Kishikawa, M., Hirose, H., Amano, Y., Izumi, N., Miwa, Y., and Ohno, S. (2004) *Curr. Biol.* **14,** 1425–1435
32. Hamaguchi, A., Suzuki, E., Murayama, K., Fujimura, T., Hikita, T., Iwabuchi, K., Handa, K., Withers, D. A., Masters, S. C., Fu, H., and Hakomori, S. (2003) *J. Biol. Chem.* **278,** 41557–41565
33. Ren, J., Datta, R., Shioya, H., Li, Y., Oki, E., Biedermann, V., Bharti, A., and Kufe, D. (2002) *J. Biol. Chem.* **277,** 33758–33765
34. Bailey, K., Cook, H. W., and McMaster, C. R. (2005) *Biochim. Biophys. Acta.* **1733,** 199–209
35. Frasch, S. C., Henson, P. M., Kailey, J. M., Richter, D. A., Janes, M. S., Fadok, V. A., and Bratton, D. L. (2000) *J. Biol. Chem.* **275,** 23065–23073
36. Greene, M. W., Ruhoff, M. S., Roth, R. A., Kim, J. A., Quon, M. J., and Krause, J. A. (2006) *Biochem. Biophys. Res. Commun.* **349,** 976–986
37. Duran, A., Diaz-Meco, M. T., and Moscat, J. (2003) *EMBO J.* **22,** 3910–3918
38. Ryu, J., Hah, J. S., Park, J. S., Lee, W., Rampal, A. L., and Jung, C. Y. (2002) *Arch. Biochem. Biophys.* **403,** 71–82
39. Nishikawa, K., Toker, A., Johannes, F. J., Songyang, Z., and Cantley, L. C. (1997) *J. Biol. Chem.* **272,** 952–960
40. House, C., and Kemp, B. E. (1987) *Science* **238,** 1726–1728
41. Kunkel, M. T., Garcia, E. L., Kajimoto, T., Hall, R. A., and Newton, A. C. (2009) *J. Biol. Chem.* **284,** 24653–24661
42. Violin, J. D., and Newton, A. C. (2003) *IUBMB Life* **55,** 653–660
43. Li, L., Lorenzo, P. S., Bogi, K., Blumberg, P. M., and Yuspa, S. H. (1999) *Mol. Cell. Biol.* **19,** 8547–8558
44. Qi, X., and Mochly-Rosen, D. (2008) *J. Cell Sci.* **121,** 804–813
45. Nguyen, T., Ogbi, M., and Johnson, J. A. (2008) *J. Biol. Chem.* **283,** 29831–29840
46. Liu, J., Liao, Z., Camden, J., Griffin, K. D., Garrad, R. C., Santiago-Pérez, L. I., González, F. A., Seye, C. I., Weisman, G. A., and Erb, L. (2004) *J. Biol. Chem.* **279,** 8212–8218
47. Lakshmi, S., and Joshi, P. G. (2006) *Neuroscience* **141,** 179–189
48. Bilbao, P. S., Santillán, G., and Boland, R. *Arch Biochem. Biophys.* (2010) **499,** 40–48
49. Peterson, T. S., Camden, J. M., Wang, Y., Seye, C. I., Wood, W. G., Sun, G. Y., Erb, L., Petris, M. J., and Weisman, G. A. *Mol. Neurobiol* (2010) **41,** 356–366
50. Kunkel, M. T., and Newton, A. C. (2010) *J. Biol. Chem.* **285,** 22748–22752

SUPPLEMENTAL FIGURE 1. **Localization of PKC δ-RFP, C2-deleted PKC δ-RFP, and nuclear-localized PKC δ-RFP.**
PKC δ-RFP, C2-deleted PKC δ-RFP (PKC δ(ΔC2)-RFP), and nuclear localized PKC δ-RFP (Nuc-PKC δ-RFP) were expressed in HeLa cells and observed using confocal laser scanning microscopy. Bars, 10 μm.

SUPPLEMENTAL FIGURE 1